



Cite this: *Dalton Trans.*, 2024, **53**, 12043

Received 6th May 2024,
Accepted 23rd June 2024

DOI: 10.1039/d4dt01331j

rsc.li/dalton

High ionic conduction in a robust anionic metal–organic framework containing Mg^{2+} under guest vapors†

Shintaro Niwa,^a Shuhei Hashimoto,^a Duotian Chen,^b Takashi Toyao,^{id b}
Ken-ichi Shimizu^{id b} and Masaaki Sadakiyo^{id *a}

We report on the synthesis and high ionic conductivity of a highly crystalline Mg^{2+} -containing metal–organic framework (MOF) with Type A feature (*i.e.*, anionic framework having Mg^{2+} as a counter cation). We synthesized $\text{Mg}[\text{Zr}(\text{C}_{14}\text{H}_3\text{O}_8)_2]$ (SU-102-Mg) through ion exchange reaction. SU-102-Mg showed a high ionic conductivity of $3.6 \times 10^{-5} \text{ S cm}^{-1}$ (25 °C, under MeCN vapor).

Solid-state ionic conductors have attracted much attention because they are potentially applicable as electrolytes for high-performance secondary batteries.¹ Especially, the migration of magnesium ions (Mg^{2+}) is one of the challenging issues in improving the performance of the rare-element-free secondary battery.² However, the migration of Mg^{2+} in solids is more difficult compared to that of monovalent ionic carriers because of the strong electrostatic interaction with neighboring anions.³ Therefore, the number of reports on Mg^{2+} conductors operating at ambient temperature is still very much limited.

Conversely, metal–organic framework (MOF)-based ionic conductors have recently been extensively developed because of their highly regular and designable pores, which could act as ion-conducting pathways for various ionic carriers.^{4,5} In the case of the Mg^{2+} carrier, we recently found that MOFs containing Mg^{2+} carriers in the pores exhibit drastic enhancement of ionic conductivity under the vapor of small organic guest molecules (*e.g.*, MeCN), termed vapor-induced ionic conduction.⁶ It is also reported that the Mg^{2+} -containing MOFs are classified into two types (*i.e.*, Type A: Mg^{2+} carriers introduced as counter cations of the anionic framework; Type B: Mg^{2+} carriers introduced as Mg^{2+} salts).⁴ So far, several examples of Type B compounds showing superionic conductivity under the

vapor of optimal guest molecules have been reported.^{6–8} Although Type A compounds, prepared through ion exchange reaction, potentially have advantages when applied to the secondary battery (*e.g.*, high transport number), only one compound, MOF-688-Mg, which exhibits low crystallinity, has been reported to date.⁹ Because its conductivity ($1.3 \times 10^{-5} \text{ S cm}^{-1}$, 25 °C)⁹ is still much lower than that of Type B compounds (*e.g.*, MIL-101 $\supset \{\text{Mg}(\text{TFSI})_2\}_{1.6}$: $1.9 \times 10^{-3} \text{ S cm}^{-1}$, 25 °C),⁷ the further development of Type A compounds is highly desired.

Here, we report on a highly crystalline Mg^{2+} -conducting MOF with Type A feature. We succeeded in preparing a Mg^{2+} -containing porous MOF, $\text{Mg}[\text{Zr}(\text{C}_{14}\text{H}_3\text{O}_8)_2]$ (SU-102-Mg), through a simple ion exchange reaction by employing a robust anionic framework, SU-102,¹⁰ as the mother framework (Fig. 1). We found that SU-102-Mg shows high crystallinity even after the ion exchange with Mg^{2+} and a high ionic con-

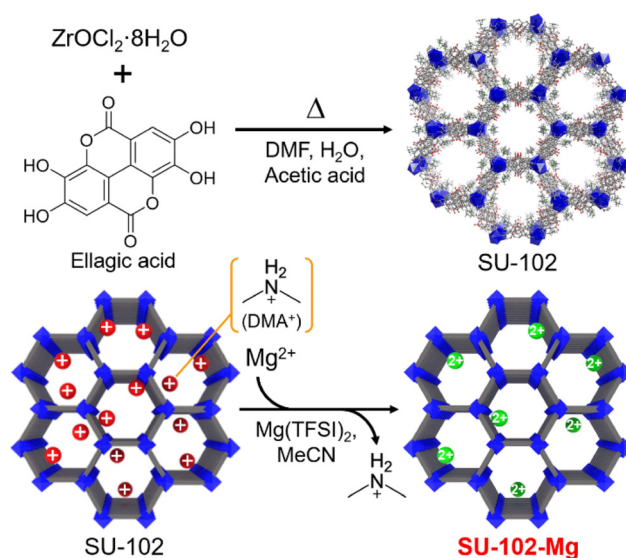


Fig. 1 Synthetic scheme of the crystalline Mg^{2+} -containing anionic MOF through ion-exchange reaction.

^aDepartment of Applied Chemistry, Faculty of Science Division I, Tokyo University of Science, 1-3 Kagurazaka, Shinjuku-ku, Tokyo 162-8601, Japan.
E-mail: sadakiyo@rs.tus.ac.jp

^bInstitute for Catalysis, Hokkaido University, Sapporo, Hokkaido 001-0021, Japan

† Electronic supplementary information (ESI) available: Details of synthesis and physical measurements; NMR spectra; TGA curves; Nyquist plots; adsorption isotherms; conductivity; IR spectra. See DOI: <https://doi.org/10.1039/d4dt01331j>



ductivity of $3.6 \times 10^{-5} \text{ S cm}^{-1}$ at room temperature (RT) under MeCN vapor. Detailed analysis of the guest adsorption, ionic conductivity, and infrared (IR) spectroscopy revealed that the significant increase in ionic conductivity is derived from the formation of coordinated Mg^{2+} carriers, which is similar to the case of the previously reported Mg^{2+} salt-containing MOF.⁷

Following previous literature,¹⁰ the mother MOF, SU-102 ($(\text{DMA})_2[\text{Zr}(\text{C}_{14}\text{H}_3\text{O}_8)_2]$), an anionic MOF with dimethyl ammonium (DMA^+) as the counter cations in its pores, was synthesized by the typical solvothermal method with Zr^{4+} and ellagic acid as the ligand (details are shown in the ESI†). Samples were characterized with X-ray powder diffraction (XRPD) and N_2 adsorption isotherms. As shown in Fig. 2 and 3, the porous mother MOF was successfully synthesized. For the prepared SU-102, Mg^{2+} carriers were introduced in the pores instead of the included DMA^+ through an ion exchange reaction in MeCN solution of Mg salt, $\text{Mg}(\text{TFSI})_2$ (TFSI^- = bis(trifluoromethanesulfonyl)imide) (see the ESI†). After the reaction, the sample was carefully washed with pure MeCN to remove the remaining $\text{Mg}(\text{TFSI})_2$.

The presence of Mg^{2+} in the ion-exchanged sample, SU-102-Mg, was confirmed by inductively coupled plasma-atomic emission spectroscopy (ICP-AES). The measurement revealed that the Mg^{2+} was stoichiometrically introduced (1.0 Mg^{2+} per formula, instead of two DMA^+) in the pores to form $\text{Mg}[\text{Zr}(\text{C}_{14}\text{H}_3\text{O}_8)_2]$. The exchange of DMA^+ was also confirmed by ^1H NMR. As shown in Fig. S1,† the peaks from the DMA^+ cations completely disappeared after the ion exchange reaction, indicating the absence of DMA^+ in SU-102-Mg. The good agreement of the elemental analysis for SU-102-Mg also confirmed the stoichiometric ion exchange (see the ESI†).

The crystal structure of the Mg^{2+} -containing MOF, SU-102-Mg, was characterized with XRPD measurements. As shown in Fig. 2, SU-102-Mg showed sharp peaks, evidencing its high crystallinity even after inclusion of Mg^{2+} . The XRPD pattern of SU-102-Mg is almost the same as that of SU-102, clearly indicating that SU-102-Mg had no significant changes in its funda-

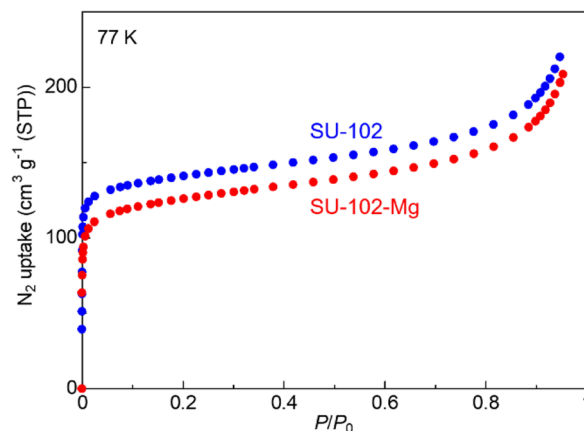


Fig. 3 N_2 adsorption isotherms of SU-102-Mg and SU-102, measured at 77 K.

mental framework structure. Note that the intensity ratio is slightly different between the samples before and after the ion exchange reaction. This should be due to the change in electron density inside the pores of the MOF, which is consistent with the fact that the stoichiometric ion exchange from DMA^+ to Mg^{2+} occurred in the pores of the sample. As shown in Fig. S2,† the thermal stability of SU-102-Mg is also similar to that of SU-102.

To confirm the porosity of the prepared MOF, we measured adsorption isotherms at 77 K. Fig. 3 shows the adsorption isotherms of the samples before and after the ion exchange. SU-102-Mg showed a large amount of adsorption at the low-pressure region, resulting in a typical Type I isotherm. This clearly indicates that the SU-102-Mg has apparent porosity even after the inclusion of Mg^{2+} ions in the pores. The BET surface area of SU-102-Mg was estimated to be $461 \text{ m}^2 \text{ g}^{-1}$, which is similar to that of SU-102 ($519 \text{ m}^2 \text{ g}^{-1}$), indicating that the high porosity remained after the ion exchange. This is consistent with the fact that SU-102-Mg has fundamentally the same framework structure, as shown in the XRPD results. As mentioned, we previously reported an example of a Mg^{2+} -containing MOF with Type A feature (MOF-688-Mg). However, it showed low crystallinity and no apparent porosity in the N_2 adsorption measurements. In this study, we succeeded in creating a crystalline porous Mg^{2+} -containing MOF with Type A feature through ion exchange reaction. Since the crystalline nanopores often act as excellent ion-conducting pathways, the ionic conductivity is strongly expected to be promoted. In addition, the high porosity would be advantageous in vapor-induced ionic conduction because of the high capability to accept the guest molecules that enhance the migration of Mg^{2+} .

To reveal the ionic conductivity of the crystalline MOF containing only Mg^{2+} in its pores, we performed alternating current impedance measurements under various conditions (Fig. 4, S3, and Table S1†). Fig. 4 shows the temperature dependence of ionic conductivity under various guest vapors of small organic molecules or dry N_2 . As with a previous report

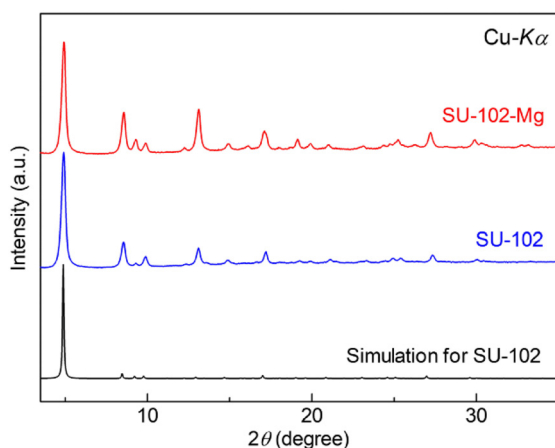


Fig. 2 XRPD patterns of SU-102-Mg and SU-102 and simulated pattern of SU-102.



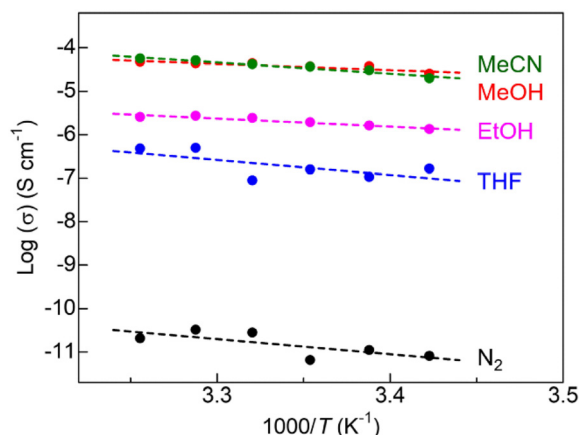


Fig. 4 Temperature dependence of the ionic conductivity of SU-102-Mg under (green) MeCN, (red) MeOH, (pink) EtOH, and (blue) THF vapors, compared to (black) dry N₂.

(MOF-688-Mg),⁹ SU-102-Mg exhibited insulating character under dry N₂, clearly indicating that Mg²⁺ located in the pores are strongly bound by the framework and thus cannot be migrated. Conversely, small guest molecules such as MeOH and MeCN drastically enhance its ionic conductivity. This is also similar to the case of MOF-688-Mg. The ionic conductivity of SU-102-Mg reaches 3.6×10^{-5} S cm⁻¹ at 25 °C under the optimal guest (MeCN) vapor, which is almost three times higher than that of MOF-688-Mg (1.3×10^{-5} S cm⁻¹ at 25 °C under MeCN vapor) and is the highest value among the Mg²⁺-containing MOFs with the Type A feature. The result suggested that the crystalline pores or regular channels of SU-102-Mg deeply contribute to the efficient migration of the included Mg²⁺. As listed in Table S1,[†] the activation energy of SU-102-Mg under each guest is also similar to that of MOF-688-Mg,⁹ suggesting the similar conducting mechanisms under the guest vapors.

Previously, we reported that the drastic increase of ionic conductivity in Mg²⁺-containing MOFs under guest vapor (*i.e.*, vapor-induced Mg²⁺ conduction) is derived from the formation of coordinated Mg²⁺ carriers with high mobility. To gain information about the mechanism of the vapor-induced Mg²⁺ conduction in SU-102-Mg, firstly, we evaluated the guest adsorption property of SU-102-Mg for the optimal guest, MeCN. As shown in Fig. S4,[†] SU-102-Mg adsorbed a large amount of MeCN from the low-pressure region, finally reaching approximately six molecules per formula. Next, we evaluated the vapor pressure dependence of ionic conductivity (Fig. S5[†]). The ionic conductivity deeply depends on MeCN vapor pressure and increased with increasing pressure, confirming that the adsorbed MeCN molecules truly enhanced the Mg²⁺ conduction in SU-102-Mg. By combining these data, we could reveal the relationship between ionic conductivity and the number of adsorbed guest molecules (Fig. S6[†]). Fig. S6[†] clearly indicates that the ionic conductivity did not obviously increase at low MeCN content, but started to slightly increase at around 4 adsorbed MeCN molecules per formula (*i.e.*, per one Mg²⁺). It continuously increased to reach the maximum conductivity

above 10^{-5} S cm⁻¹ at around the maximum MeCN content of approximately 6 molecules per formula. Compared with our previous study on the Type B compound, Mg²⁺ salt-containing MOF (MIL-101 ⊃ {Mg(TFSI)₂}_{1.6}),⁷ the tendency of this relationship is actually very similar. In the case of MIL-101 ⊃ {Mg(TFSI)₂}_{1.6}, the conductivity is drastically increased at around 9.6 MeCN molecules per formula, which corresponds to 6-coordination to Mg²⁺, forming the highly mobile coordinated carriers.⁷ Considering this fact, the similar behavior of SU-102-Mg (Fig. S6[†]) is indicative that the increase of ionic conductivity in SU-102-Mg was caused by the change in mobility of the included Mg²⁺ due to the formation of the coordinated carriers. It is also suggested that one of the main reasons for the relatively low ionic conductivity of SU-102-Mg ($\geq 10^{-5}$ S cm⁻¹) compared to MIL-101 ⊃ {Mg(TFSI)₂}_{1.6} ($\geq 10^{-3}$ S cm⁻¹)⁷ is the limited pore capacity of SU-102-Mg: 6 MeCN molecules per Mg²⁺ does not seem enough to make the formed carriers highly mobile (*i.e.*, still not free from the electrostatic interaction from the anionic framework). We believe that the additional guest molecules (*i.e.*, more than 6), coordinating to the framework, play a critical role in reducing the remaining electrostatic interaction to allow the formed carriers to migrate more freely.

To confirm the formation of the coordinated Mg²⁺ carriers in SU-102-Mg, we measured the *in situ* Fourier transform infrared (FT-IR) spectra under MeCN vapor (Fig. S7[†]). In the case of SU-102 (without Mg²⁺), the main peaks at around 2255 and 2283 cm⁻¹ are attributable to CN stretching mode (ν_2) and the combination of CH₃ bending and CC stretching mode ($\nu_3 + \nu_4$), respectively.¹¹ In contrast, SU-102-Mg showed apparently shifted peaks at around 2289 and 2315 cm⁻¹, which should be attributed to ν_2 and $\nu_3 + \nu_4$ bands, derived from the MeCN molecules coordinating to metal ions (Mg²⁺).¹¹ This behaviour is similar to the previously reported Mg²⁺ salt-containing MOF,⁷ although SU-102-Mg shows some extra peaks that would be attributed to MeCN molecules with various coordination forms (*e.g.*, other than the typical octahedral six-coordination). This result clearly confirmed the existence of the coordinated Mg²⁺ carriers in the pores under MeCN vapor and is consistent with the results of conductivity and adsorption measurements described above. These results confirm that the adsorbed small guest molecules act as the conducting media for Mg²⁺ conduction and indeed help the migration of Mg²⁺ carriers located in the MOF pores.

Conclusions

In conclusion, we demonstrated the high ionic conductivity of a highly crystalline Mg²⁺-containing MOF with Type A feature. The prepared MOF, SU-102-Mg, showed an ionic conductivity of 3.6×10^{-5} S cm⁻¹ at 25 °C under MeCN vapor, which is almost three times higher than the previously reported Type A compound with low crystallinity. We also revealed that the drastic enhancement of ionic conductivity under the guest vapor is derived from the formation of the highly mobile co-



ordinated Mg^{2+} carriers, as is the case with Type B compounds. These results provide useful information towards the development of MOF-based Mg^{2+} conductors.

Data availability

All the data used is demonstrated in the manuscript and ESI.†

Conflicts of interest

There are no conflicts to declare.

Acknowledgements

This work was partly supported by the Joint Usage/Research Center for Catalysis, Nippon Sheet Glass Foundation for Materials Science and Engineering, Tokuyama Science Foundation, JSPS KAKENHI No. 21K05089, and JST FOREST No. JPMJFR2110.

References

- 1 S. Randau, D. A. Weber, O. Kötz, R. Koerver, P. Braun, A. Weber, E. Ivers-Tiffée, T. Adermann, J. Kulisch, W. G. Zeier, F. H. Richter and J. Janek, Benchmarking the performance of all-solid-state lithium batteries, *Nat. Energy*, 2020, **5**, 259–270.
- 2 D. Aurbach, Z. Lu, A. Schechter, Y. Gofer, H. Gizbar, R. Turgeman, Y. Cohen, M. Moshkovich and E. Levi, Prototype systems for rechargeable magnesium batteries, *Nature*, 2000, **407**, 724–727.
- 3 S. Ikeda, M. Takahashi, J. Ishikawa and K. Ito, Solid electrolytes with multivalent cation conduction. 1. Conducting species in Mg-Zr-PO_4 system, *Solid State Ionics*, 1987, **23**, 125–129.
- 4 M. Sadakiyo and H. Kitagawa, Ion-conductive metal-organic frameworks, *Dalton Trans.*, 2021, **50**, 5385–5397.
- 5 D.-W. Lim and H. Kitagawa, Proton Transport in Metal-Organic Frameworks, *Chem. Rev.*, 2020, **120**, 8416–8467.
- 6 Y. Yoshida, K. Kato and M. Sadakiyo, Vapor-Induced Superionic Conduction of Magnesium Ions in a Metal-Organic Framework, *J. Phys. Chem. C*, 2021, **125**, 21124–21130.
- 7 Y. Yoshida, T. Yamada, Y. Jing, T. Toyao, K. Shimizu and M. Sadakiyo, Super Mg^{2+} Conductivity around $10^{-3} \text{ S cm}^{-1}$ Observed in a Porous Metal-Organic Framework, *J. Am. Chem. Soc.*, 2022, **144**, 8669–8675.
- 8 K. Aoki, K. Kato and M. Sadakiyo, High Mg^{2+} conduction in three-dimensional pores of a metal-organic framework under organic vapors, *Dalton Trans.*, 2023, **52**, 15313–15316.
- 9 S. Niwa and M. Sadakiyo, Preparation of a Mg^{2+} -containing MOF through ion exchange and its high ionic conductivity, *Dalton Trans.*, 2022, **51**, 12037–12040.
- 10 E. S. Grape, A. J. Chacón-García, S. Rojas, Y. Pérez, A. Jaworski, M. Nero, M. Åhlén, E. Martínez-Ahumada, A. E. G. Feindt, M. Pepillo, M. Narongin-Fujikawa, I. A. Ibarra, O. Cheung, C. Baresel, T. Willhammar, P. Horcajada and A. K. Inge, Removal of pharmaceutical pollutants from effluent by a plant-based metal-organic framework, *Nat. Water*, 2023, **1**, 433–442.
- 11 O. Kristiansson, FT-IR, Investigation of Acetonitrile- D_3 -Cation Interactions, *Spectrosc. Lett.*, 1999, **32**, 783–792.

